

Methotrexate
and
MSU-H MSNs

Materials and Methods

Mesoporous material MSU-H was procured from Sigma-Aldrich, USA and used for drug loading procedure without further purification. MSU-H material was characterized by different instrumental techniques.

6.1 Characterization

The mesostructured MSU-H MSNs were characterized by various instrumental techniques, to get important information about different physicochemical features:

6.1.1 Scanning electron microscopy (SEM)

The morphology of MSU-H MSNs was examined by scanning electron microscopy operated at an acceleration voltage of 10 kV. The samples were attached to aluminum stubs with double side adhesive carbon tape then gold coated and examined using a scanning electron microscope, Leo 1430 VP-Germany.

6.1.2 Transmission electron microscopy (TEM)

A high resolution electron microscopic image of the mesoporous MSU-H MSNs was taken with a JEOL JEM-2100 electron microscope-USA, equipped with a pole piece, operated at 120 kV. The powder samples were grounded softly in mortar and dispersed in ethanol in an ultrasonic bath for several minutes. A few drops were then deposited on 200 mesh copper grids covered with a holey carbon film. The electron micrographs were recorded in electron negative films and in a digital PC system attached to the electron microscope.

6.1.3 FTIR analysis

MSU-H MSNs (25 mg) was mixed with dry KBr (300 mg) and ground to a finely divided powder, loaded into a 13 mm die, and pressed under 6000 psi pressure for 5 min. to obtain a pellet. This technique avoids excessive grinding which might cause structural degradation. All measurements were performed at ambient temperature to keep the hydration state of the samples constant and to minimize any structural changes. The spectra were recorded in the range of 4000 cm^{-1} - 700 cm^{-1} using a Bruker alpha T, Fourier-Transform Infrared Spectrometer- Germany.

6.1.4 Powder X-ray diffraction (XRD)

Mesoporous MSU-H MSNs was evaluated using an X'Pert- MPD powder X-ray diffraction spectrometer, Philips- Netherland. In all cases, the generator was operated at 40 kV and 30 mA. In order to avoid the problem of illuminated area at low 2θ angles, all the samples were measured using the same sample holder. The MSNs samples were scanned from 1 to 9 of diffraction angle (2θ) at scanning speed of $0.02\ 2\theta/5\text{s}$.

6.1.5 Nitrogen adsorption-desorption isotherm (BET surface analysis)

Nitrogen adsorption- desorption isotherms were determined using a computer controlled Micromeritics ASAP 2010-USA apparatus. Prior to adsorption

measurements, the MSU-H MSNs was degassed under vacuum overnight at 423 K. The specific surface area was determined by application of the BET method⁵ to the isotherm.

6.2 Drug-Methotrexate loading in MSU-H MSNs

MSU-H MSNs were used for drug loading process. MSNs were dried in oven at 100 °C for 30 min in order to remove moisture from the pores. The drug loading was carried out by direct impregnation method. The MSNs was placed as powder into the drug solution of the drug with a given concentration. The drug loading procedure is described below.

In preliminary drug loading procedure, MTX (100 mg) was dissolved in an appropriate solvent (10 ml) and then MSU-H MSNs (200 mg) was added. The mixture was kept under magnetic stirring at room temperature for 24h and then was left to settle for 2h to allow the sedimentation of the fine precipitate that was collected by filtration. The recovered solid was dried for 24h under vacuum at room temperature and stored at room temperature.

The drug loaded MSNs were analyzed by XRD, nitrogen adsorption isotherm, surface area, FT-IR spectroscopy and DSC analysis. The loading efficiency (LE) within the MSU-H MSNs was determined indirectly by determining the amount of non-entrapped or non-adsorbed drug, by measuring concentration of MTX in the solvent and in the washing solutions. The drug loading efficiency was analyzed spectrophotometrically (Shimadzu-1700, Japan) at 306 nm. Suitable dilution factor was applied and the loading efficiency was calculated according to the formula¹ given below.

$$Wt\% = \frac{m_1 - \frac{50}{v} CV}{m_2 + \left(m_1 - \frac{50}{v} CV \right)} \times 100$$

Where, m_1 and m_2 correspond to the initial mass of MTX and mesoporous materials added into 0.1 M HCl solution. C is the concentration of filtrates diluted in 50 ml volumetric flask, v is sampled volume from filtrates, and V is the volume of 0.1 M HCl solution for drug loading.

6.2.1 Optimization of drug loading procedure

The process of drug loading was optimized with respect to solvent, drug: carrier ratio, temperature, time, and stirring rate.

□ Solvent

Solvent optimization involves the use of different solvents for drug loading and was checked for % of drug load. The main selection criterion was that the solvent should give optimum solubility of drug and minimum or no solubilization of carrier. As different solvents give different pH atmosphere so indirectly, optimization of solvents also covers the optimization of pH.

□ Ratio of drug and drug carrier

Another important parameter is to select proper ratio of drug (MTX) and drug carrier (MSU-H) for maximum entrapment. Different ratio were tried and checked for drug loading.

□ Temperature and time

Temperature and soaking/stirring time are two important parameters which may affect drug loading. Drug loading procedure was carried out at two different temperature i.e. room temperature and 40° C. Similarly, five different time durations were selected i.e. 6h, 12h, 24h, 48h, and 72h, for drug loading process.

□ Stirring rate

Rate of stirring also greatly affect the drug loading, hence it is important to optimize the stirring rate. Effect of stirring at higher and normal rate is studied by using magnetic stirrer.

6.2.2 Factorial design for drug loading optimization

3³ factorial design was used to determine the effect of the three independent factors: the concentration of drug solution, the stirring rate, and drug: carrier weight ratio on the % drug loading of MSU-H MSNs. Each factor was tested at three levels of low, medium and high, designed as -1, 0, and +1 respectively.

Microsoft Excel was used for multiple regression calculation in order to deduce the factors having significant effect on the formulation properties. Three-dimensional response surface plots and two dimensional contour plots resulting from equations were obtained by the NCSS software.

6.2.3 Evaluation of drug loaded MSU-H MSNs

Drug loaded MSNs were evaluated by similar instrumental techniques as described in section 6.1.

6.3 *In-Vitro* dissolution study

In-vitro drug release from the MSNs was studied by the rotating paddle method at 50 rpm (Veego dissolution test apparatus-basket type USP), 37 ± 0.5 °C and in sink conditions. Tests were performed in the following dissolution media⁷: simulated gastric fluid at pH 1.2 ± 0.1 , phosphate buffer at pH 4.5 ± 0.1 , phosphate buffer at pH 6.8 ± 0.1 and simulated intestinal fluid at pH 7.4 ± 0.1 . Drug release was monitored for 1h and compared to MTX crystalline powder, the physical mixture and market formulation. Five milliliters of dissolution fluid was removed from the vessel at predetermined intervals and replaced by the same volume of fresh dissolution medium. The samples were filtered through PTFE 0.45 μm filters and MTX content was determined by UV spectrophotometry (λ max = 303 nm for pH 1.2, λ max = 303 nm for pH 4.5, λ max = 374 nm for pH 6.8, λ max = 372 nm for pH 7.4). All experiments were performed in triplicate and the error was expressed as standard deviation.

Results and Discussion

MSU-H MSNs were procured commercially and the material was characterized by different instrumental techniques. The characterization results revealed that the MSU-H MSNs were of prescribed standard².

6.4 Characterization of MSU-H MSNs

6.4.1 Electron microscopy (SEM and TEM)

Figure 6.1 represents the morphology of the MSU-H MSNs observed on SEM. It could be seen that all samples were regular spheres with smooth surface (diameters <20 nm). TEM observations revealed the presence of mesoporous structure with a characteristic hexagonal honeycomb pattern arrangement of the channels (Fig. 6.2). The TEM images of MSU-H MSNs revealed the presence of disconnected channels arranged in a 2-D hexagonal pattern.

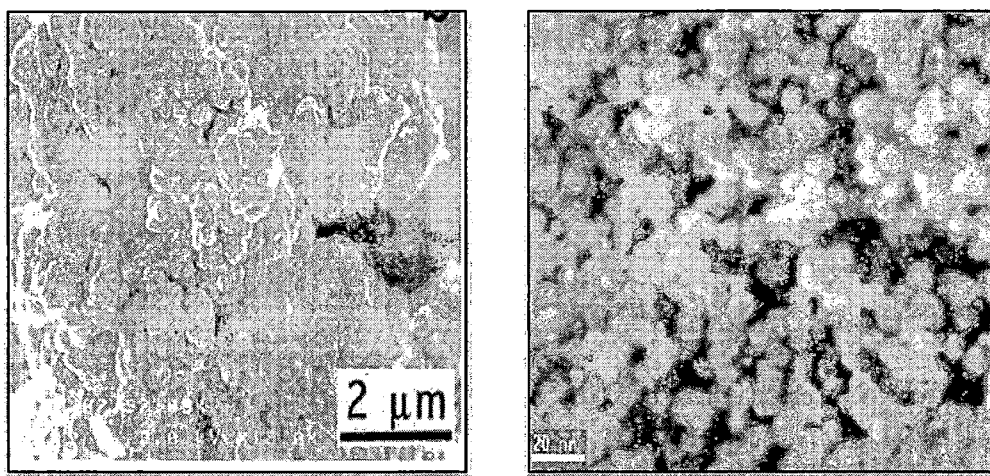


Figure 6.1: SEM images of MSU-H MSNs

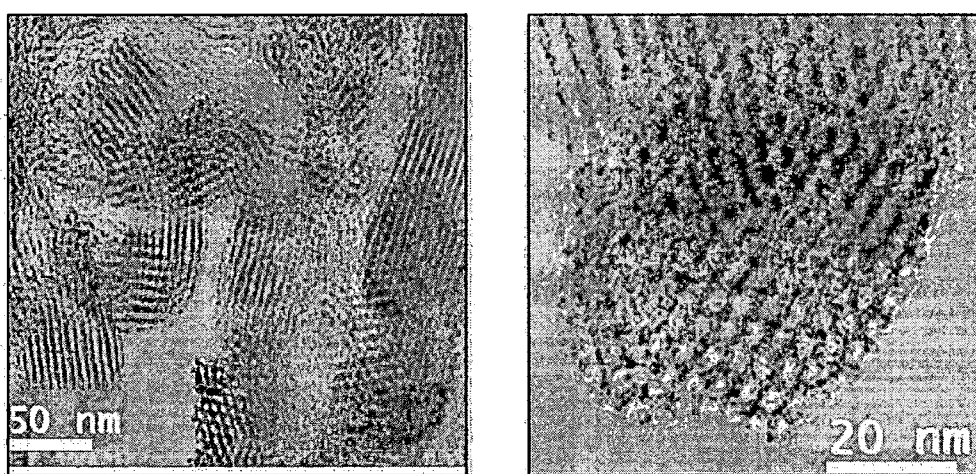


Figure 6.2: TEM images of MSU-H MSNs

6.4.2 FTIR analysis

Potassium bromide diluted MSU-H samples were analyzed by FTIR. FTIR spectrum of MSU-H (Fig. 6.3) showed the presence of a vibration band at 3747 cm^{-1} attributable to isolated terminal silanol groups and of another large band at 3452 cm^{-1} attributable to geminal and associated terminal silanol groups. The stretching vibrations of Si-O-Si and Si-OH can be seen at 1083 and 968 cm^{-1} .

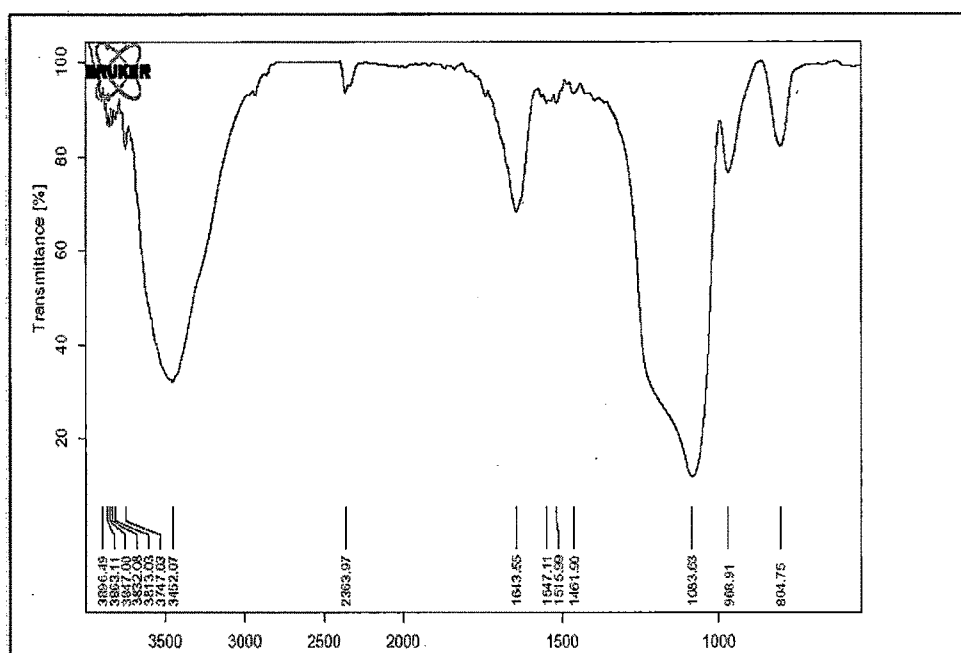


Figure 6.3: FTIR spectra of synthesized MSU-H MSNs

6.4.3 Powder X-ray diffraction (XRD)

The MSNs samples were scanned at diffraction angle (2θ) value from 0.5 to 4 at scanning speed of 0.02 $2\theta/5\text{s}$. Small angle XRD pattern of MSU-H MSNs is shown in Fig. 6.4. MSU-H MSNs diffractogram showed typical reflections^{2,3} of mesostructure. It can be seen that XRD pattern of MSU-H MSNs presents a strong (100) diffraction peak with two small (110) and (200) diffraction peaks, confirming the uniform pore channels and the formation of highly ordered 2D hexagonal mesostructures.

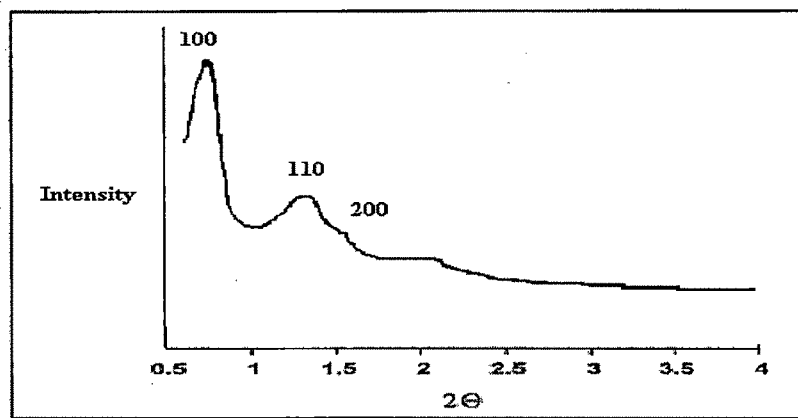


Figure 6.4: XRD pattern of MSU-H MSNs

6.4.4 Nitrogen adsorption-desorption isotherm (BET surface analysis)

Prior to adsorption measurements, the MSU-H MSNs were degassed under vacuum overnight at 423 K. The inflection of the capillary condensation observed at a P/P_0 value of about 0.6 for the adsorption isotherms. The isotherms of MSU-H MSNs were stepped like type IV isotherms, very similar to that of MCM-41 MSNs reported in 5.5.4. The abrupt step in the $P/P_0 = 0.6-0.8$ region implies the existence of mesopores.

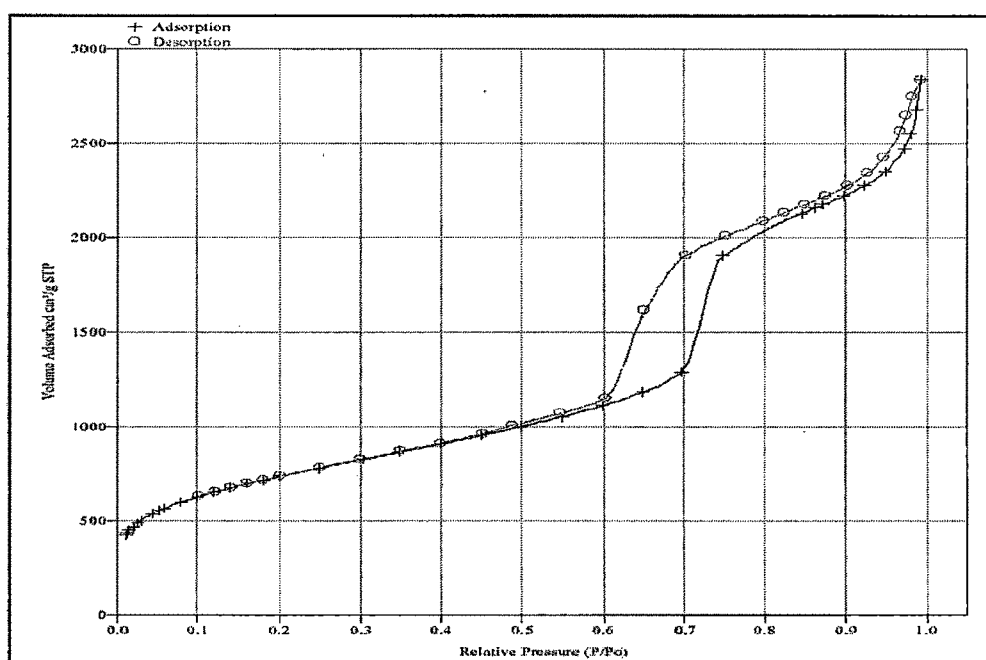


Figure 6.5: Nitrogen adsorption/desorption isotherms of MSU-H MSNs

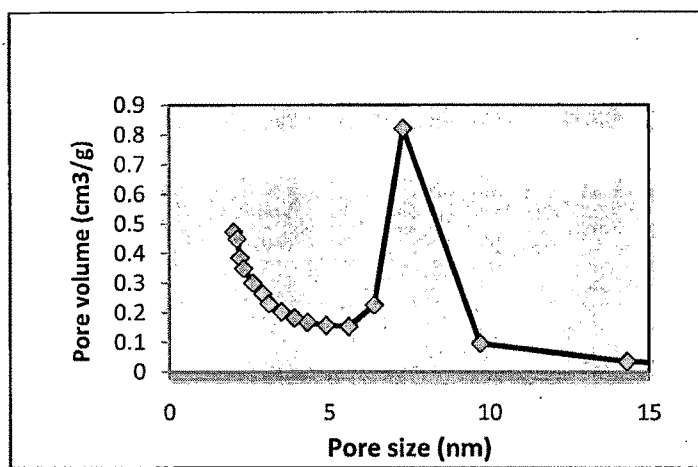


Figure 6.6: Pore size distribution of synthesized MSU-H MSNs

Table 6.1: Pore diameter, volume and BET surface area of MSU-H MSNs

MSNs	Pore diameter (nm)	Pore volume (cm ³ /g)	S _{BET} (m ² /g)
MSU-H	7.291	0.821	644.021

Nitrogen adsorption-desorption isotherms of MSU-H MSNs are shown in Fig. 6.5. MSU-H MSNs shows typical type IV isotherm according to IUPAC classification represents the mesoporosity of the nanoparticles. The isotherm recorded for MSU-H MSNs also shows a hysteresis loop at high relative pressure, which has been ascribed to the presence of interparticle porosity⁴. The calculated B.E.T. specific surface area for MSU-H was 644 m²/g. The average pore size distribution and mesopore volume for MSU-H MSNs was found to 7.29 nm (Fig. 6.6) and 0.821 cm³/g respectively. Numerical data shown in Table 6.1.

6.5 Drug-Methotrexate loading in MSU-H MSNs

Due to the high specific areas and pore volumes of MSNs, large quantities of drug can be incorporated into the porous MSNs by adsorption to the pore or/and surface of MSNs. The MSU-H MSNs was placed into a concentrated solution of the MTX and stirred for about 24h, for maximum diffusion of the drug molecules into the mesopores (Fig. 6.7).

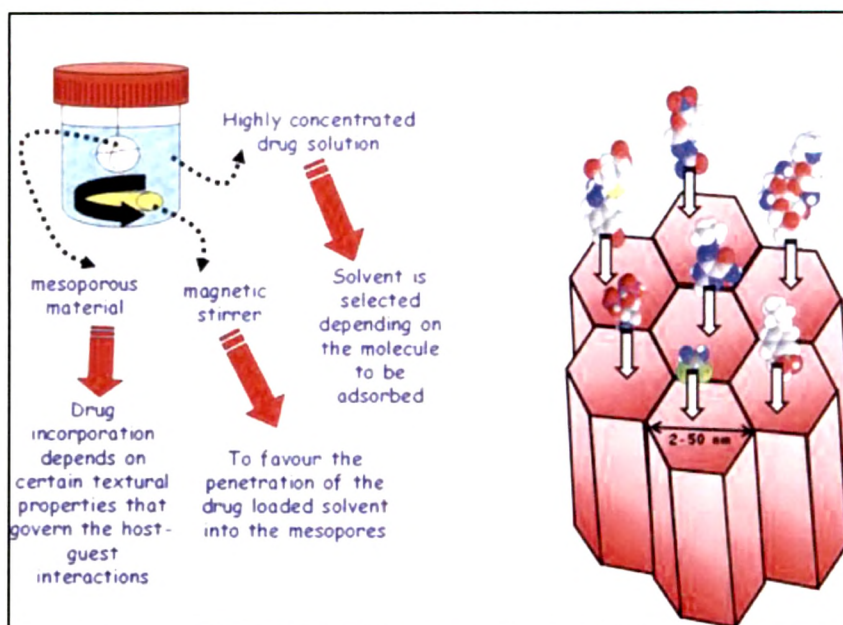


Figure 6.7: Schematic representation of the drug loading procedure

The drug loading process is influenced by several factors which include solvents, ratio of drug and drug carrier (MSNs), temperature, time and stirring rate. Other factors which can affect the drug loading are the mesoporosity of the MSNs and pore size as it determines the size of the molecules which can be adsorbed into the mesopores.

It is important to know whether drug molecules are adsorbed in the pores or on the surface of MSNs as it can later on affect the release characteristics. Normally, pore/drug size ratio >1 allows the adsorption of drug inside the pores⁵. It was found that the molecular size of MTX is ~ 2.3 nm⁶ and the data of nitrogen adsorption isotherm suggested the pore size of MSU-H MSNs was 7.2 nm. If we calculate the ratio by equation given above the value was found to be 3.13, indicating that, MTX molecules can easily be confined within the pores.

The drug loading into the MSU-H MSNs is also controlled by the chemical nature of the pores and pore walls. The inorganic networks of MSU-H MSNs have plenty of silanol groups (Si-OH), present into the mesopores and on the surface (Fig. 6.8) that would interact (through hydrogen bond) with the functional groups of the drug. Attracting interaction between the silanol group of MSNs and functional group of the drug, the drug molecules either confined within the pores or they adsorbed to the surface of MSNs.

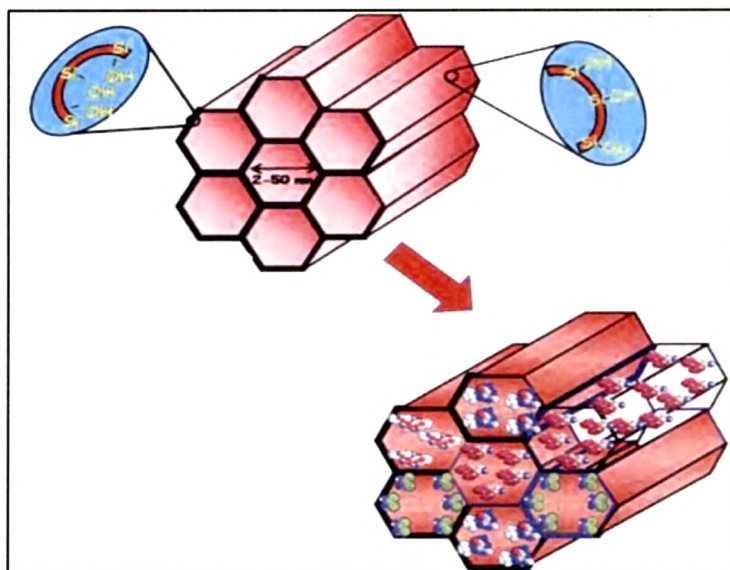


Figure 6.8: Textural properties and drug loading and/or adsorption on MSNs

The probable mechanism of drug loading is that, the a carboxylic acid group of MTX would form hydrogen bonds with the silanol groups of MSU-H MSNs and consequently drug molecules would be retained into the mesopores (Fig. 6.9).

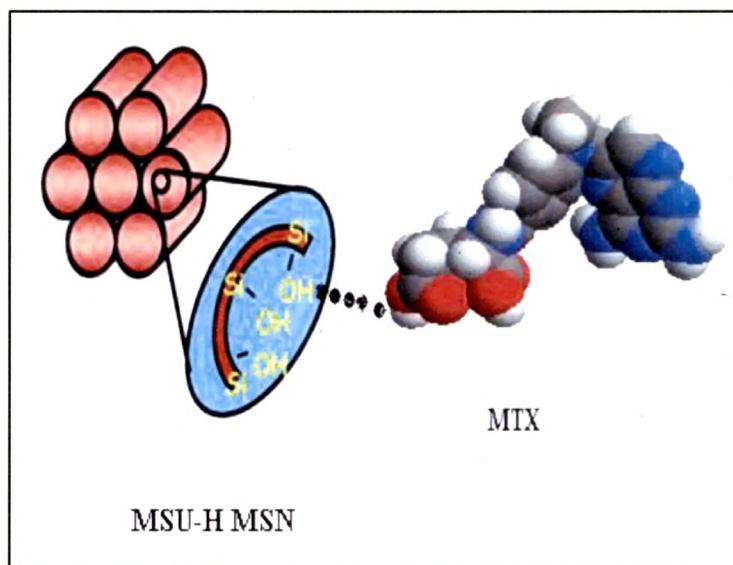


Figure 6.9: MTX linkage to silanol group of MSU-H MSNs

To observe the influence of the different factors, the drug loading process was optimized for solvent, ratio of drug and drug carrier (MSNs), temperature, time and stirring rate, in following section.

6.5.1 Optimization of drug loading procedure

□ Solvent

The first prerequisite for a loading solvent is a sufficient solubility of the drug in it. The optimal solvent for the loading process might not be the one in which the solubility is the highest. It is often a sign of strong attractive interactions between the solvent and the solute⁷, and it may cause the solute to prefer staying in the solution phase to adsorption onto the carrier. Another inauspicious situation in drug loading is the competitive adsorption; if the solvent possesses attractive interactions with the adsorbent, it will compete on the adsorption sites with the solute. Besides the affinities among the solute, solvents and adsorbent surface, also the possible degradation of the API (active pharmaceutical ingredient) in the solvent must be taken into account. Even if the API would not decompose, it may re-crystallize from the solution as a different polymorph or as a solvate. Solvents that induce the degradation of the API must be avoided. In addition, the use of many solvents is limited by their toxicity or too low or too high volatility.

For the present study three solvents were tried. As MTX is soluble in solutions of mineral acids and in dilute solutions of alkali hydroxides, 0.1 M HCl and 0.1 M NaOH were selected as solvents. Dimethyl formamide was another solvent checked for drug loading. Drug loading was carried out with these selected solvents and % LE was checked, results are shown in Table 6.2 and presented in Fig. 6.10.

Table 6.2: Effects of different solvents on MSU-H MSNs drug loading

Solvent used for drug loading	pH of the medium	% Drug loading in MSU-H MSNs
Dimethyl formamide	6.8	41.965
0.1 M HCl	1.2	48.969
0.1 M NaOH	12.5	10.658

Results of % LE was suggest that the 0.1 M HCl is appropriate solvent for the drug loading, as it provide maximum loading with comparison to 0.1 M NaOH and dimethyl formamide. Optimizations of solvents also cover the optimization of pH for the loading process. The data of loading process suggested that acidic media is more suitable for effective entrapment of MTX in MSU-H MSNs.

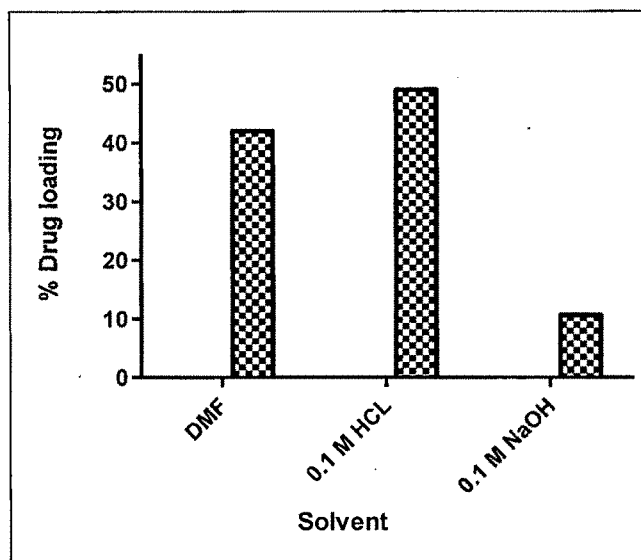


Figure 6.10: Effects of different solvents on MSU-H MSNs drug loading

□ *Ratio of drug and drug carrier*

Ratio of drug to MSNs can greatly affects drug loading ability. It was necessary to find out the optimum drug to MSNs ratio. To optimize the ratio, different proportion of MSNs to drug was taken as mentioned in Table 6.3.

Table 6.3: Effects of drug: MSNs ratio on MSU-H MSNs drug loading

Weight Ratio Drug : Carrier	% Drug loading in MSU-H MSNs
1: 0.5	47. 980
1:1	48. 608
1: 1.5	35. 851
1: 2	38. 677

Ratio was optimized by taking fixed proportion of drug and variable proportion of MSNs. Four different proportion were selected for MSNs, 0.5, 1, 1.5, and 2. It was found that maximum drug entrapment was achieved with 1:1 weight ratio. The optimization-data graphically present in Fig. 6.11.

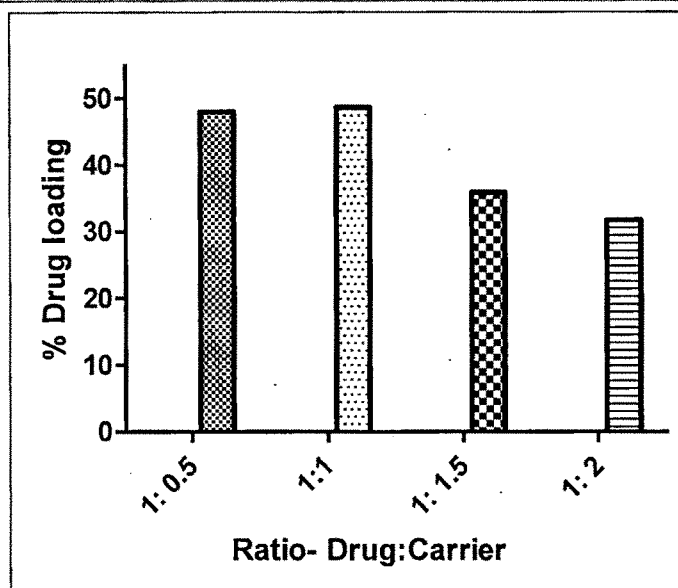


Figure 6.11: Effects of drug:MSNs ratio on MSU-H MSNs drug loading

□ *Temperature and time*

Solubility is a function of temperature. By increasing the loading temperature, the solubility of a drug can be increased. Increase in temperature may also accelerate the degradation of drug or evaporation of the solvent, and the temperature also affects the adsorption rate and equilibrium. It is also necessary to check the effect of time so loading process was conducted for different time duration.

The loading process was carried out at two different temperature i.e. room temperature and 40° C. Similarly five different time durations were selected for proper agitation during the loading process. Stirring was provided with magnetic stirrer for five different time durations, i.e. 6h, 12h, 24h, 48h, and 72h. The results are summarized in Table 6.4 and graphically presented in Fig. 6.12.

Table 6.4: Effects of temperature and time on MSU-H MSNs drug loading

Temperature	% of Drug loading at different time duration				
	6h	12h	24h	48h	72h
Room temp.	42.381	48.858	48.167	48.198	48.101
40° C	39.428	40.198	42.325	43.469	42.981

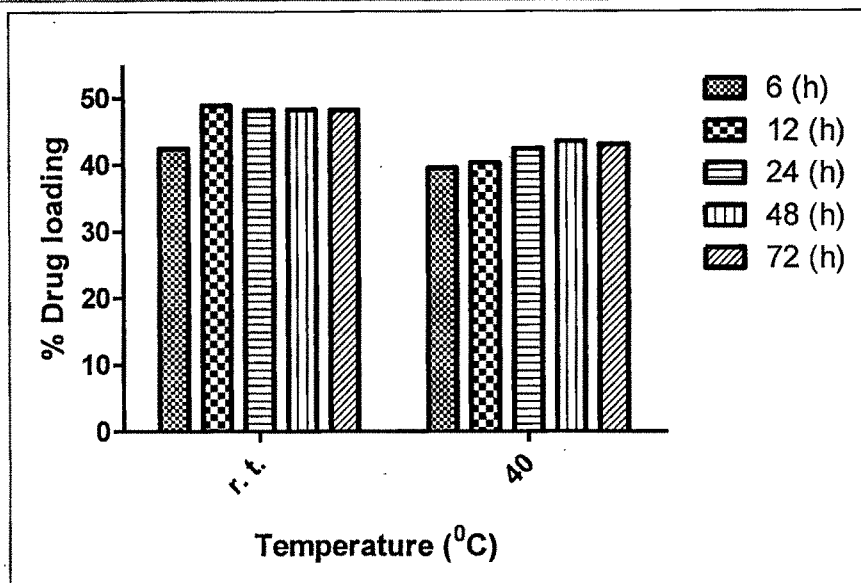


Figure 6.12: Effects of temperature and time on MSU-H MSNs drug loading

The results of % LE revealed that maximum drug loading was attainable if the MSNs and MTX were continuously agitated at least for 12h.

The results of drug loading at 40° C suggested that the elevated temperature was not suitable for the high loading. Higher temperature may increase the MTX solubilization but at elevated temperature the MTX molecules may experience high Brownian motion⁸⁻¹⁰ which may not allow the easy diffusion and adsorption in the mesopores of MSU-H MSNs. During the loading process at 40° C, it was found that MTX was crystallized out from the solution. Once MTX was crystallized, it may not effectively penetrate in to the pores but accumulated on the surface of MSNs. This crystallized MTX was likely to be removed during the washing of MSU-H MSNs and leads to poor drug loading.

□ *Stirring rate*

During the loading process, the solution was continuously magnetically stirred to improve access of the concentrated solution to the mesopores¹⁰. MSNs sample was added in drug solution with vigorous stirring and continue for 1h, followed by gentle stirring for 23h.

Vigorous stirring was provided at 800 rpm, whereas the gentle stirring rate was optimized at four levels i.e. 50 rpm, 100 rpm, 200 rpm and 400 rpm. The results are summarized in Table 6.5 and graphically presented in Fig. 6.13. The results revealed that as stirring rate was increased from 100 rpm to 400 rpm; the rate of drug loading was decreased from 49 to 31 %. Optimized stirring rate data suggested that for the maximum drug loading the stirring should be 100 rpm.

Table 6.5: Effects of stirring rate on MSU-H MSNs drug loading

Stirring speed	~50 rpm	~100 rpm	~200 rpm	~400 rpm
% Drug loading	46.547	49.107	43.628	31.629

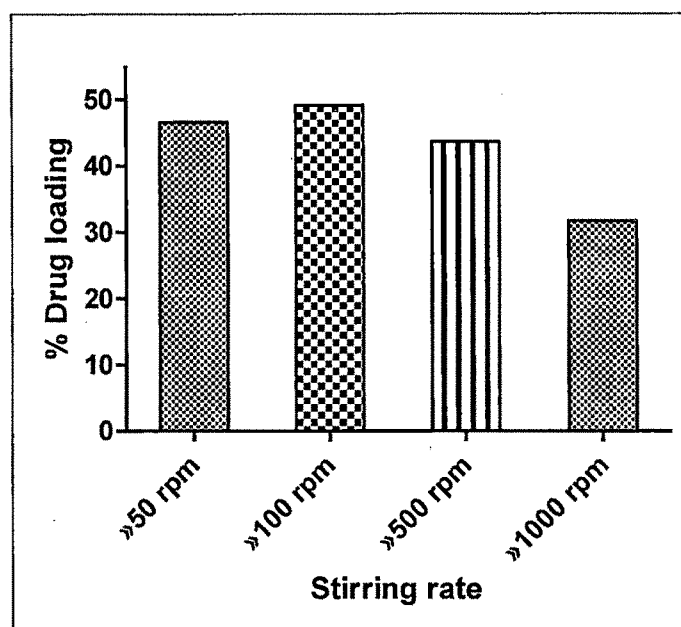


Figure 6.13: Effects of stirring rate on MSU-H MSNs drug loading

6.5.2 Factorial design for drug loading optimization

The process of drug loading was optimized with respect to different influencing variables such as solvent, ratio of drug: carrier, temperature, time, and stirring rate. The conventional method of optimization involves the study of effect of different factors on formulation by changing one variable at a time (OVAT). Since the combined effects of variables are not evaluated, it is difficult to formulate an ideal pharmaceutical formulation. It is necessary therefore to understand the complexity of process variables in development of pharmaceutical formulations using statistical analysis of each variable at a time such as factorial design¹¹.

Factorial designs involve the study of all the selected factors in all possible combinations, in a most efficient manner using minimum experiments. The effect of individual variable can be visualized with the contour plots and is very helpful to evaluate the response of different variables in optimization process. Similarly

three-dimensional response surface plots provide platform to study the effect of dependent and independent variables in formulation development.

Primary optimization data revealed that the stirring rate and ratio of drug: MSNs greatly affect the loading efficiency. A statistical model was developed to study the effect of stirring rate, weight ratio of drug: carrier and concentration of drug solution on formulation characteristics.

6.5.2.1 Preparation of batches and optimization by factorial design

Twenty-seven batches of MTX loaded MSU-H MSNs (as a carrier) were prepared using 3^3 factorial design by varying three independent variables the concentration of drug solution (X1), the stirring rate (X2), and drug: carrier ratio (X3). Each factor was tested at three levels of low, medium and high, designed as -1, 0, and +1 respectively. The normalized factor levels of independent variables are given in Table 6.6.

Table 6.6: Factorial 3^3 : factors, their levels, and transformed values

Variables with transformed value	Levels		
	Low (-1)	Medium (0)	High (1)
(X1) Concentration of drug solution (mg/ml)	1	5	10
(X2) Stirring rate (rpm)	10	50	100
(X3) Ratio drug: carrier	0.25	0.5	1

The % MTX loading efficiency (response variable) of the prepared batches was determined (Table 6.7) and the highest percent drug loading achieved in mesoporous MSU-H MSNs was 49.716% at 1 level of X1 (10 mg/ml), 1 level of X2 (100 rpm), and 1 level of X3 (1:1 weight ratio). The results were subjected to multiple-regression analysis. The fitted equation related to percent loading efficiency and transformed factors shows in Eq. (1).

$$Y = 18.651 + 11.739x_1 + 6.311x_2 + 5.220x_3 + 2.866x_1^2 + 1.020x_2^2 + 2.123x_3^2 + 1.822x_1x_2 + 3.101x_1x_3 - 1.350x_2x_3 - 2.297x_1x_2x_3$$

(1)

Table 6.7: Different batch with their experimental coded level of variables for 3³ factorial design

Batch code	X1= Concentration of drug solution	X2= Stirring rate	X3= Ratio drug: carrier	% drug loading
M1	-1	-1	-1	5.096
M2	-1	-1	0	7.974
M3	-1	-1	1	8.256
M4	-1	0	-1	7.998
M5	-1	0	0	11.698
M6	-1	0	1	13.158
M7	-1	1	-1	15.654
M8	-1	1	0	17.879
M9	-1	1	1	19.158
M10	0	-1	-1	12.569
M11	0	-1	0	13.654
M12	0	-1	1	17.321
M13	0	0	-1	18.104
M14	0	0	0	24.574
M15	0	0	1	27.951
M16	0	1	-1	21.789
M17	0	1	0	22.741
M18	0	1	1	28.025
M19	1	-1	-1	19.369
M20	1	-1	0	21.357
M21	1	-1	1	44.587
M22	1	0	-1	23.149
M23	1	0	0	25.309
M24	1	0	1	45.859
M25	1	1	-1	42.682
M26	1	1	0	45.998
M27	1	1	1	49.716

The data clearly indicated that percent loading efficiency is more dependent on the concentration of drug solution and the stirring rate than the ratio of drug: carrier. The value of correlation coefficient (r) was found to be 0.957, indicating a good fit. The small values of coefficients of terms X_2^2 , X_3^2 , X_1X_2 , X_2X_3 , and $X_1X_2X_3$ (Eq. 2), were least contributing in loading of MTX in MSU-H MSNs ($p > 0.05$). Hence, they were omitted to evolve the reduced model (Eq. 2). The summary of regression analysis is shown in Table 6.8.

$$Y = 20.747 + 11.739x_1 + 6.311x_2 + 5.220x_3 + 2.866x_1^2 + 3.101x_1x_3 \quad (2)$$

The positive sign for the coefficient of X_1 , X_2 , and X_3 in Eq. (2) showed that the percent drug loading can be increased by an increase in X_1 , X_2 , and X_3 . The results of ANOVA of the second-order polynomial equation are given in Tables 6.8.

Table 6.8: Analysis of variance (ANOVA) of variables for full and reduced model of MSU-H MSNs

	DF	SS	MS	F	R	R ²	Adj.R ²
Regression							
FM	10	3906.170	390.617	20.978	0.963	0.929	0.884
RM	5	3768.904	23.34324	37.128	0.940	0.884	0.857
Error							
FM	16	352.942	22.058				
RM	21	490.207	23.343				

$$[SSE_2 - SSE_1 = 490.207 - 352.942 = 137.265]$$

No. of parameters omitted = 5

MS of error (full model) = 22.058

$$F \text{ calculated} = (SSE_2 - SSE_1 / \text{no. of parameters omitted}) / \text{MS of error (full model)}$$

$$= (137.265 / 5) / 22.058 = 1.2445$$

Tabled F value = 2.85 ($\alpha = 0.05$, $V_1 = 5$, and $V_2 = 16$).

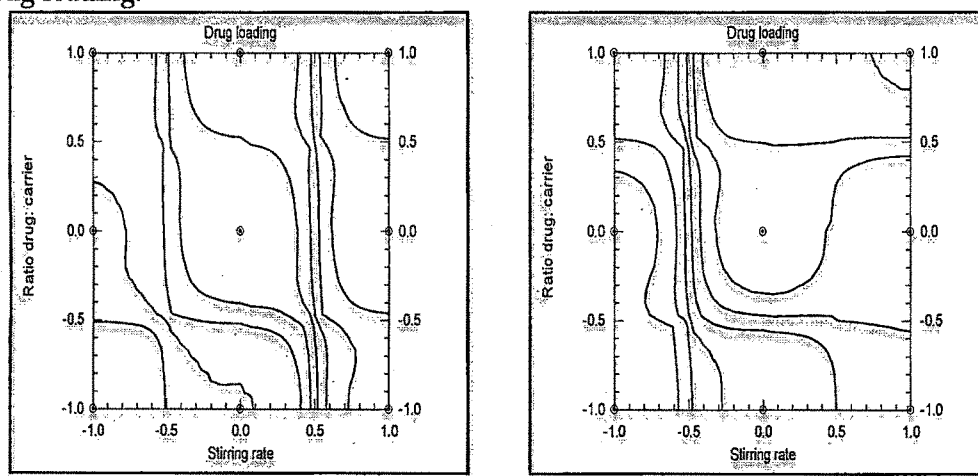
a Where DF indicates degrees of freedom; SS sum of square; MS mean sum of square and F is Fischer's ratio].

F-Statistic of the results of ANOVA of full and reduced model confirmed omission of non-significant terms of Eq. (1) and (2). Since the calculated F value (1.24) was less than the tabled F value (2.85), it was concluded that the neglected terms do not significantly contribute in the prediction.

The goodness of fit of the model was checked by the determination coefficient (R^2). In this case, the values of the determination coefficients (R^2) and adjusted determination coefficients (adj R^2) were very high (>85%), which indicates a significance of the model. All the above considerations indicate an adequacy of the regression model^{12, 13}.

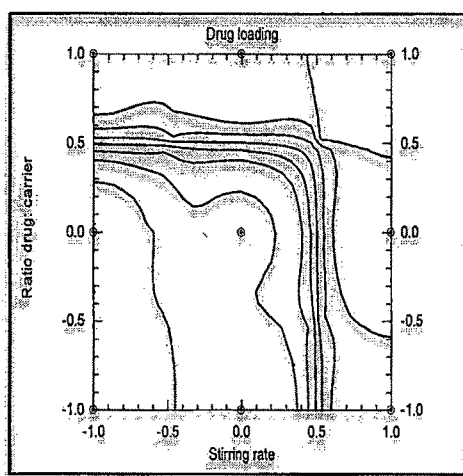
6.5.2.2 Contour plots

Fig. 6.14 (a–i) is the contour plot for MSU-H MSNs which were found to be linear and signifying linear relationship between variables X1, X2, and X3. It was observed from contour plots (Fig. 6.14-c) that maximum LE (49.716%) could be obtained with X2 between 0.5 level (50 rpm) to 1 level (100 rpm) and X3 between 0.5 level (0.5:1) to 1 level (1:1). Fig. 6.14-f revealed that maximum loading could be obtained with X1 between 0.6 level (6 mg) to 1 level (10 mg) and X3 between 0.5 level (0.5:1) to 1 level (1:1). Fig. 6.14-i showed that maximum loading could be obtained with X1 between 0.6 level (6 mg) to 1 level (10 mg) and X2 between 0.4 level (40 rpm) to 1 level (100 rpm). All the two-dimensional contour plots were found to follow the linear relationship between X1, X2, and X3 variables. From the contour, it was observed that higher drug concentration (10 mg/ml), maximum stirring rate (100 rpm), and unit ratio of drug:carrier are necessary for maximum drug loading.



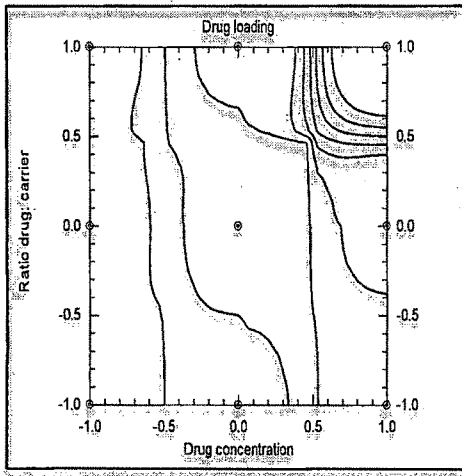
(a) Effect on LE at -1 level of X1

(b) Effect on LE at 0 level of X1

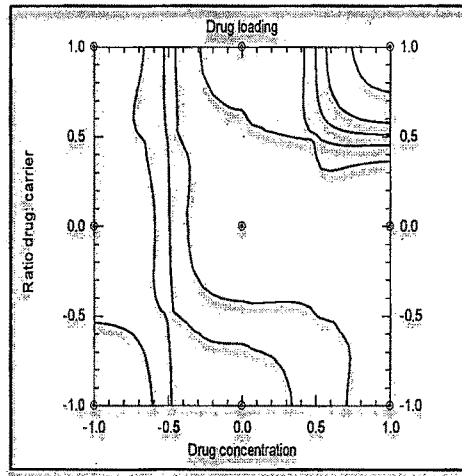


(c) Effect on LE at +1 level of X1

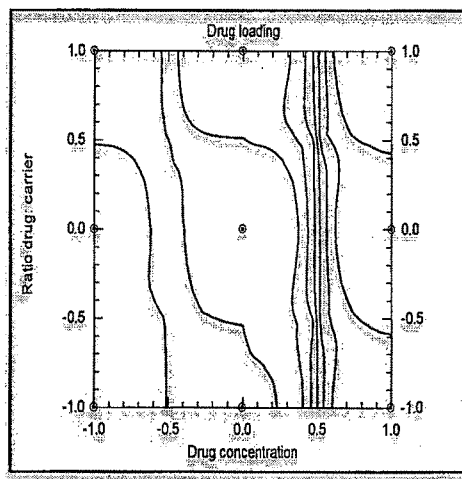
Figure 6.14 (a-c): Contour plots: Effect on LE at -1, 0 and +1 levels of drug concentration (X1)



(d) Effect on LE at -1 level of X2

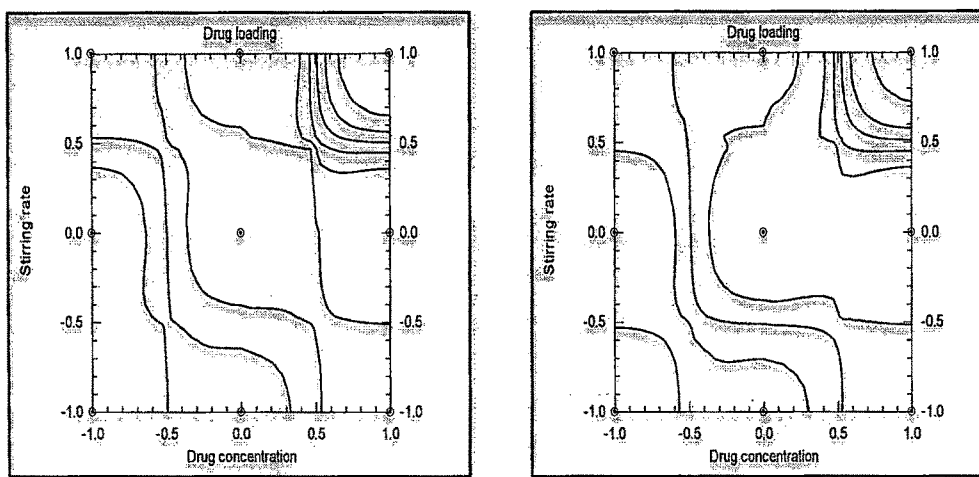


(e) Effect on LE at 0 level of X2



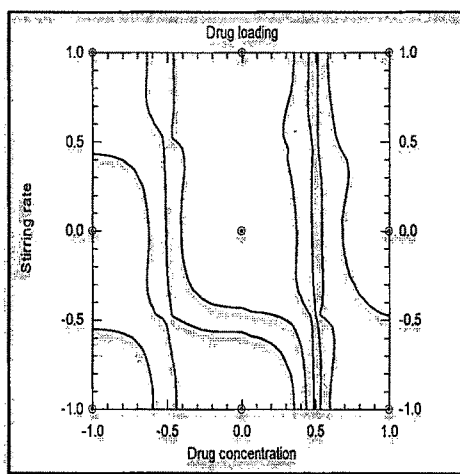
(f) Effect on LE at +1 level of X2

Figure 6.14 (d-f): Contour plots: Effect on LE at -1, 0 and +1 levels of stirring rate (X2)



(g) Effect on LE at -1 level of X3

(h) Effect on LE at 0 level of X3



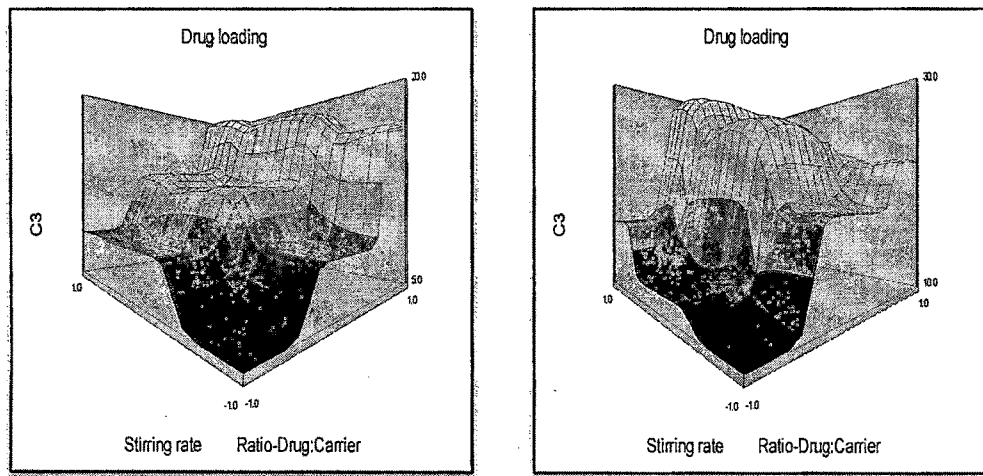
(i) Effect on LE at +1 level of X3

Figure 6.14 (g-i): Contour plots: Effect on LE at -1, 0 and +1 level of drug: carrier ratio (X3)

6.5.2.3 Response surface plots

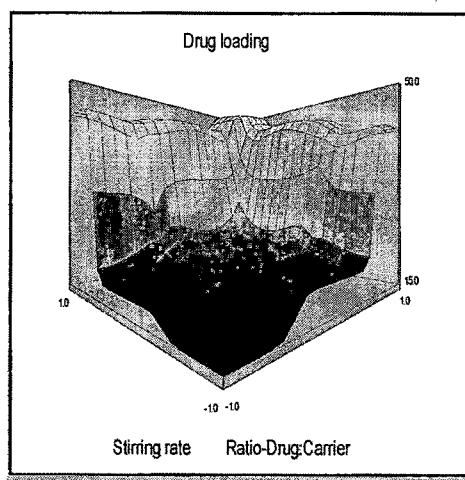
Three dimensional response surface plots generated by the NCCS software are presented in Fig. 6.15 (a-i), for MSU-H MSNs. Fig. 6.15 (a-c) depict response surface plots for LE of MSU-H MSNs at constant level of the factor X1 showing an increase in LE with increase in the stirring rate and increase in weight ratio of drug: carrier. Fig. 6.15 (d- f) depict response surface plots for LE at constant level of the factor X2 indicating an increase in LE with increase in the drug concentration and increase in weight ratio of drug: carrier. Fig. 6.15 (g-i) depict

response surface plots for LE at constant level of the factor X3 suggesting an increase in drug concentration and increase in stirring rate increases the LE.



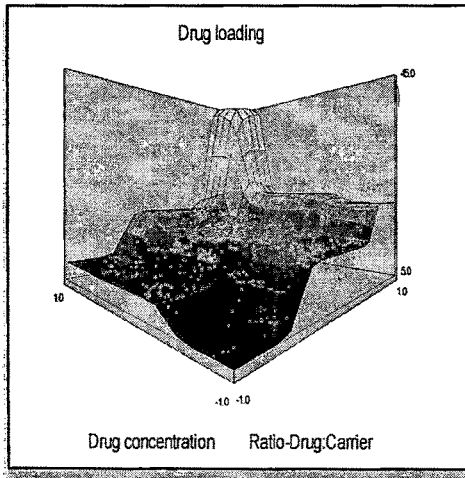
(a) Effect on LE at -1 level of X1

(b) Effect on LE at 0 level of X1

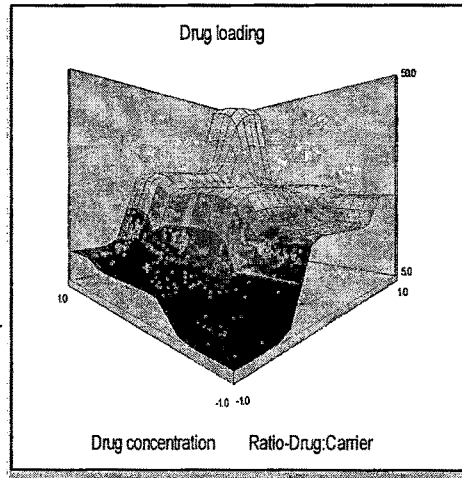


(c) Effect on LE at +1 level of X1

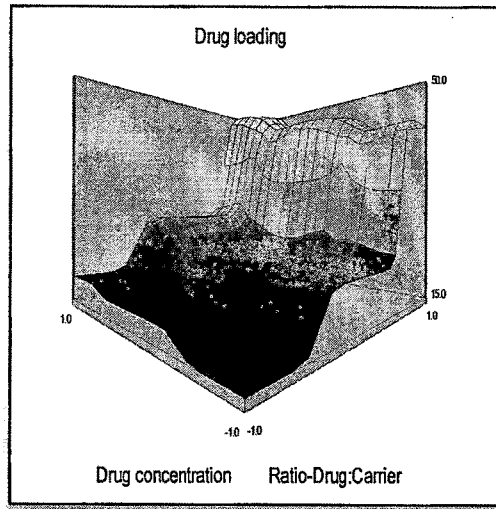
Figure 6.15 (a-c): Response surface plots: Effect on LE at -1, 0 and +1 level of drug concentration (X1)



(d) Effect on LE at -1 level of X2

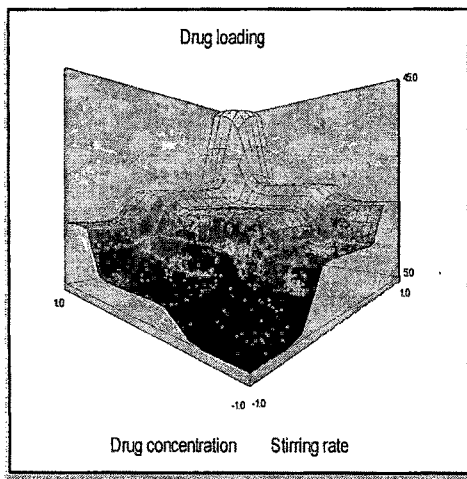


(e) Effect on LE at 0 level of X2

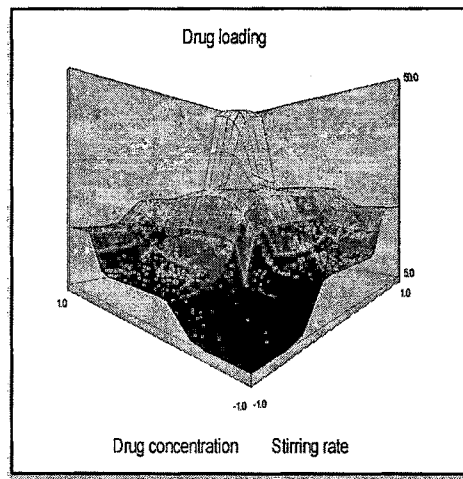


(d) Effect on LE at +1 level of X2

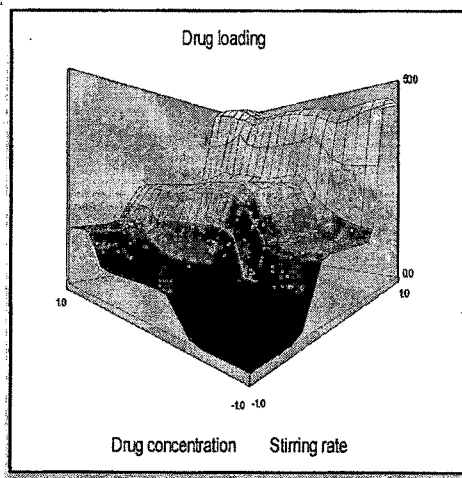
Figure 6.15 (d-f): Response surface plots: Effect on LE at -1, 0 and +1 level of stirring rate (X2)



(g) Effect on LE at -1 level of X3



(h) Effect on LE at 0 level of X3



(i) Effect on LE at +1 level of X3

Figure 6.15 (g-i): Response surface plots: Effect on LE at -1, 0 and +1 level of drug: carrier ratio (X3)

6.5.3 Evaluation of drug loaded MSU-H MSNs

Drug loaded MSNs were evaluated for maximum drug loading and intact mesoporosity. Using instrumental techniques like TEM, XRD, nitrogen adsorption, FTIR and DSC were used for this purpose.

6.5.3.1 Transmission electron microscopy (TEM)

The first step was to check that the mesostructure of the MSU-H MSNs has survived after the loading process. The MSNs sample was analyzed by TEM. The high resolution TEM images confirmed the prevalence of the ordered mesostructure after the loading step (Fig. 6.16). TEM Images are marked with some dark spots, which may be the indicative of the confinement of drug molecules within the pores.

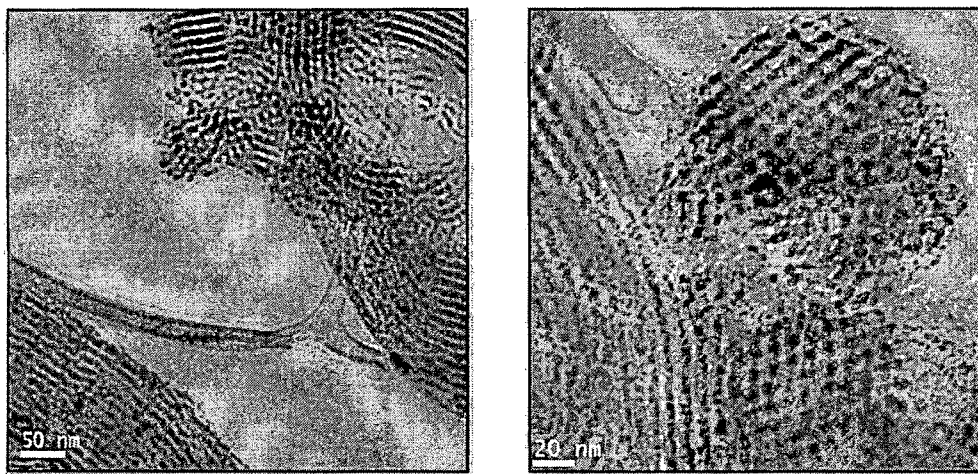


Figure 6.16: TEM images of MSU-H MSNs after drug loading

6.5.3.2 Powder X-ray diffraction (XRD)

The survival of mesoporosity of the MSNs was further confirmed by XRD. For this purpose, a small angle XRD pattern was carried out before and after the loading process (Fig. 6.17 (a-b)). The mesoporous structure of the MSU-H MSNs was confirmed by the diffraction peaks at 100 . The same characteristic diffraction peaks were observed in MSNs even after the drug loading process. Confirming that the mesostructure of MSNs was not disturbed after the drug loading. The XRD pattern of MTX is also shown in Fig. 6.17b. The drug loaded MSNs do not show the characteristic peaks of MTX further confirming the entrapment of drug molecules within the mesopores.

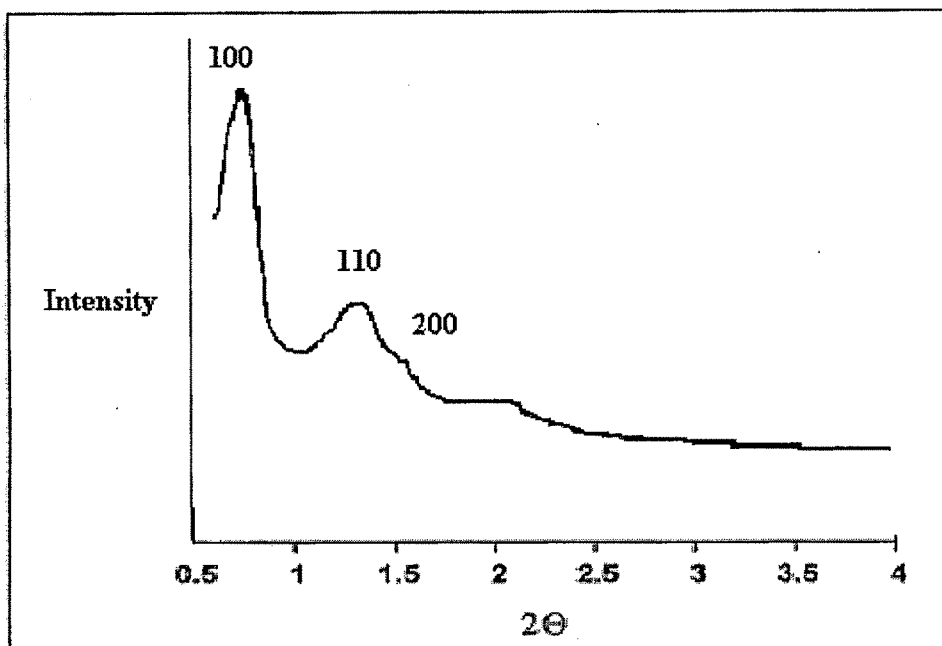


Figure 6.17-a: XRD pattern of MSU-H MSNs before the drug loading

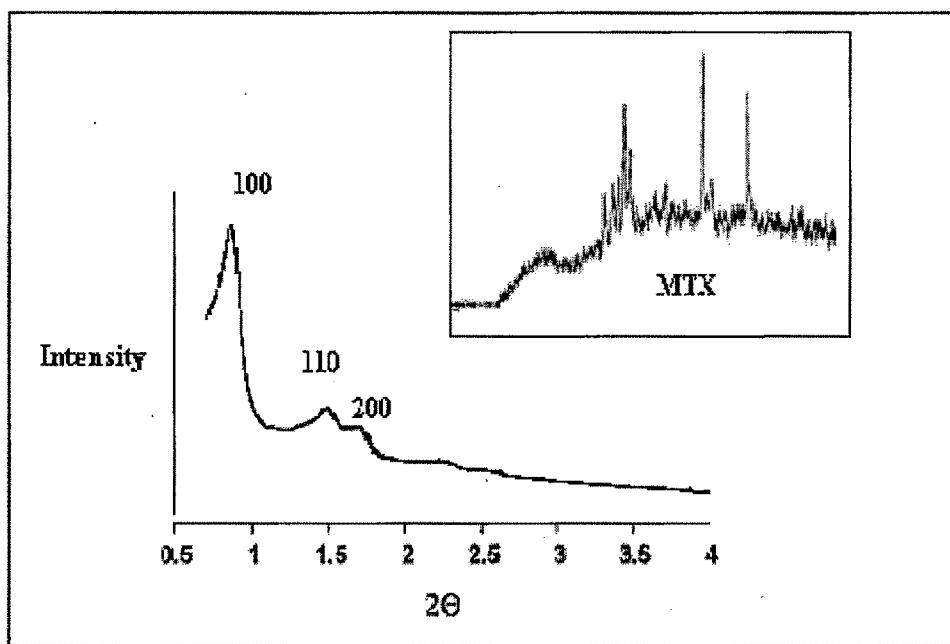


Figure 6.17-b: XRD pattern of MTX and MSU-H MSNs after the drug loading

6.5.3.3 Nitrogen adsorption isotherm (BET surface analysis)

After confirmation of the integrity of the mesostructure, next important point is to check whether the drug molecules are confined inside the mesopores or they are just on the outer surface of the MSNs. Nitrogen adsorption analysis was performed to find out the status of drug molecules. The nitrogen adsorption isotherms were obtained for the pore size distribution and the pore volume determination of MSNs, before and after the loading process.

The pore volume and surface area are normally decreased as a consequence of the MSNs–drug interaction. It was observed that the available pore volume was decreased after the drug loading indicating that the drug molecules are partially filling the mesopores, i.e. the drug molecules are being confined inside the pores¹⁴.

In Fig. 6.18 (a-b) nitrogen adsorption-desorption isotherms of MSU-H MSNs before and after the drug loading were reported. Both the isotherm of MSU-H MSNs shows typical type IV isotherm according to IUPAC classification represents the mesoporosity. The both the isotherm recorded for MSU-H MSNs also shows a hysteresis loop at high relative pressure, which has been ascribed to the presence of interparticle porosity⁴.

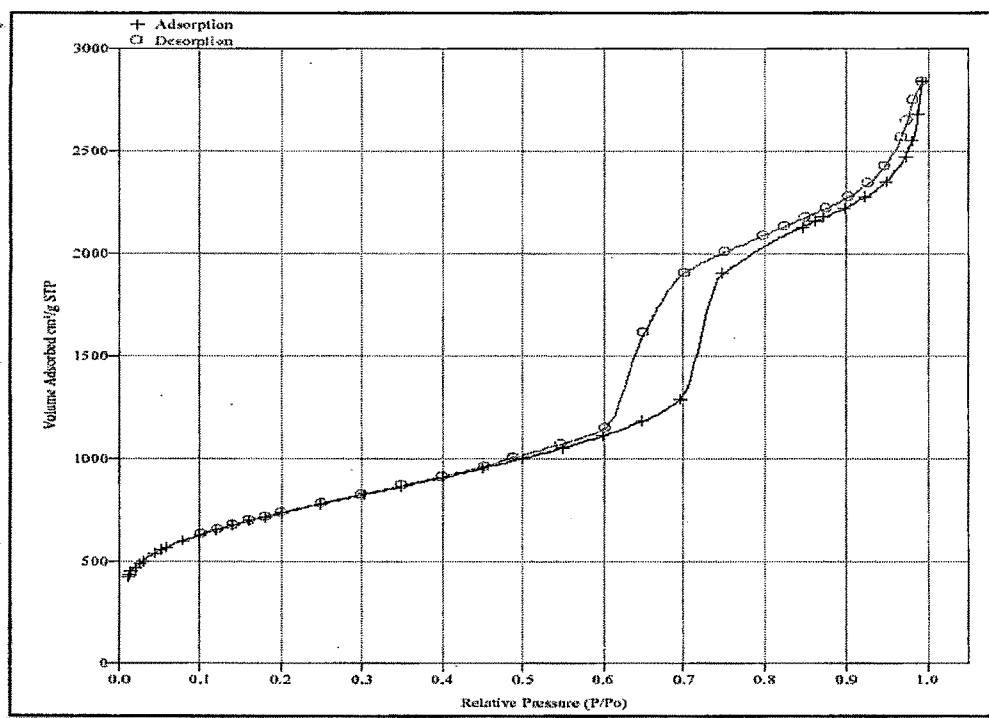


Figure 6.18-a: Nitrogen adsorption isotherm of MSU-H MSNs before the drug loading

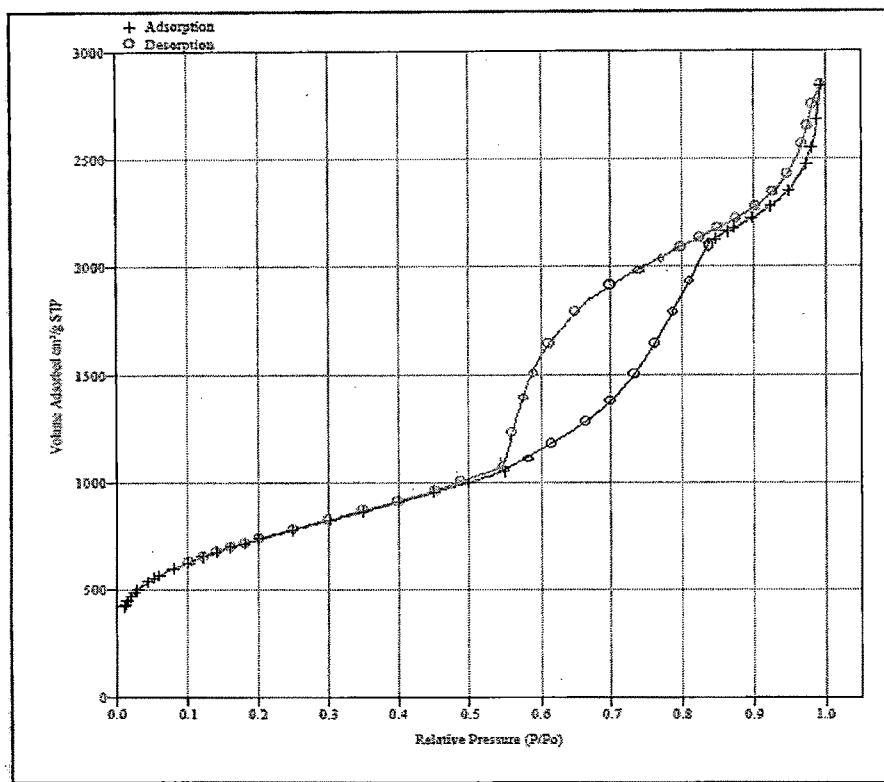


Figure 6.18-b: Nitrogen adsorption isotherm of MSU-H MSNs after the drug loading

The calculated B.E.T. specific surface area for MSU-H MSNs alone and MSU-H MSNs after MTX loading were found to be 644.02 and 236.47 m²/g, respectively. The adsorption isotherms of MTX loaded MSNs showed that the adsorbed nitrogen volume decreased after drug loading. Correspondingly, the average pore size distribution for drug loaded MSU-H MSNs, calculated by the BJH-KJS method, was shifted from 7.29 nm to 5.66 nm and the mesopore volume decreased from 0.821 to 0.509 cm³/g for the primitive MSU-H MSNs and drug loaded MSU-H MSNs, respectively (Fig. 6.19). Numerical data are shown in Table 6.9 for MSU-H MSNs and drug loaded MSU-H MSNs.

Table 6.9: Pore diameter, volume and BET surface area of MSU-H MSN

MSNs	Pore diameter (nm)	Pore volume (cm ³ /g)	S _{BET} (m ² /g)
MSU-H	7.291	0.821	644.021
MTX loaded MSU-H	5.668	0.509	236.474

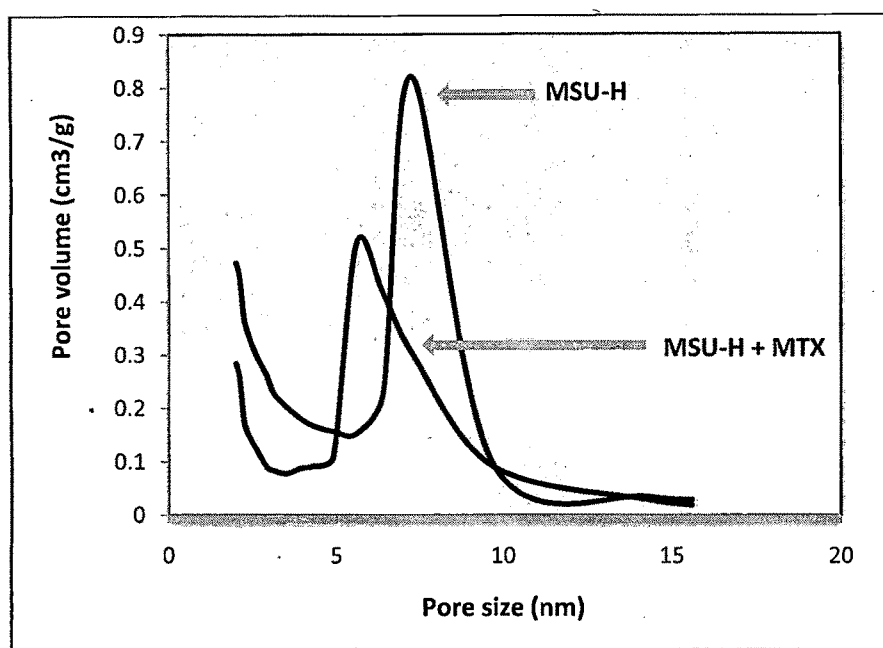


Figure 6.19: Pore size distribution and pore volume of MSU-H MSN before and after drug loading

6.5.3.4 FTIR analysis

FTIR spectrum of MSU-H MSNs (Fig. 6.21) showed the presence of a vibration band at 3747 cm⁻¹ attributable to isolated terminal silanol groups and of another large band at 3452 cm⁻¹ attributable to geminal and associated terminal silanol groups. The stretching vibrations of Si-O-Si and Si-OH can be seen at 1083 and 968 cm⁻¹. The FTIR spectral analysis of MTX powder (Fig. 6.20) showed the principal peaks at about 1682 cm⁻¹ (-COOH), 1639 cm⁻¹ (-CO-NH), 1541, 1489 cm⁻¹ (aryl system), and 825 cm⁻¹ (aromatic ring system) confirming the purity of the drug. The spectra of drug loaded MSU-H MSNs (Fig. 6.22) shows a remarkable absence of the characteristic peak observed in pure MTX sample, suggesting that majority of MTX was entrapped in MSNs.

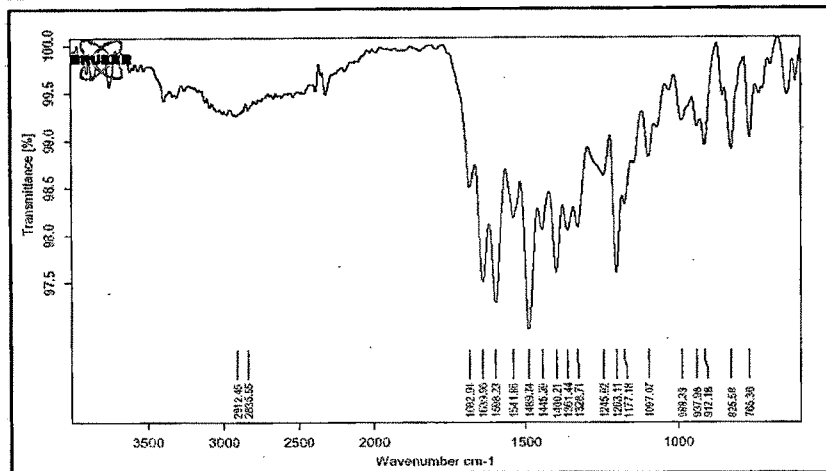


Figure 6.20: FTIR spectra of MTX

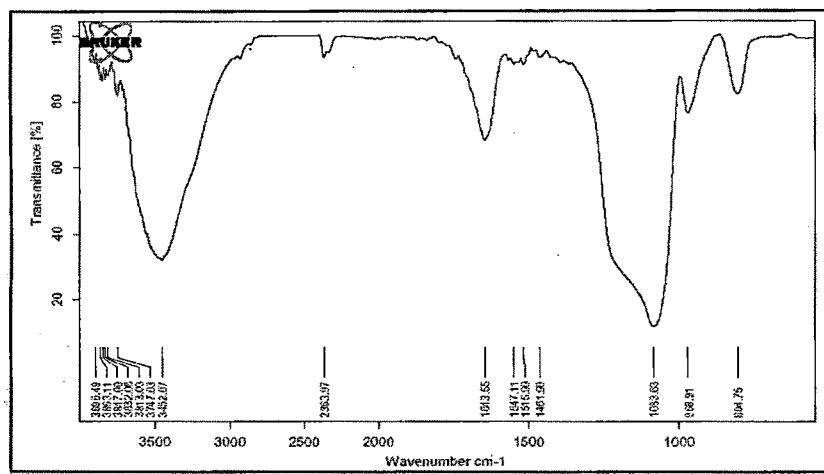


Figure 6.21: FTIR spectra of MSU-H MSNs

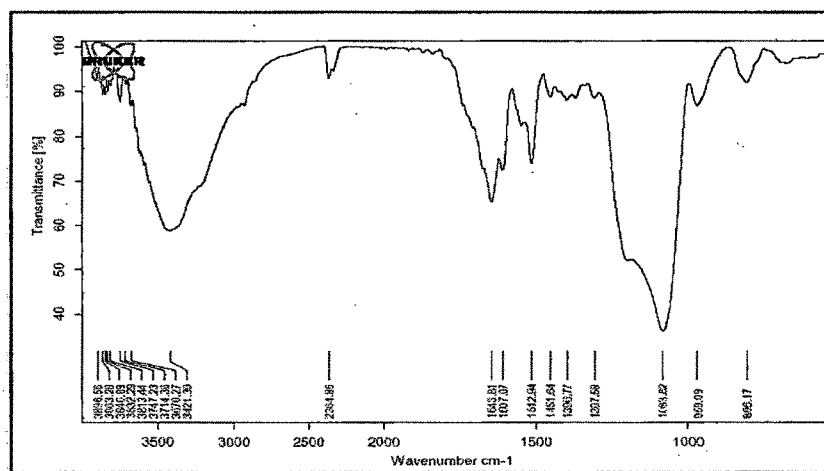


Figure 6.22: FTIR spectra of MTX loaded MSU-H MSNs

6.5.3.5 Differential scanning calorimetry (DSC)

DSC can give information whether the drug is in an amorphous form as it is entrapped within the pores or it is partially crystallized onto the external surface of MSNs. The possible surface fraction can be detected using DSC, which detects all their actions and phase transitions which are associated with enthalpy changes. If any crystalline particles exist on the surface, they appear as a melting endotherm on the DSC scan. The absence of endothermic peak in drug loaded MSNs is the indicative of the amorphous state as drug is confined within the pores.

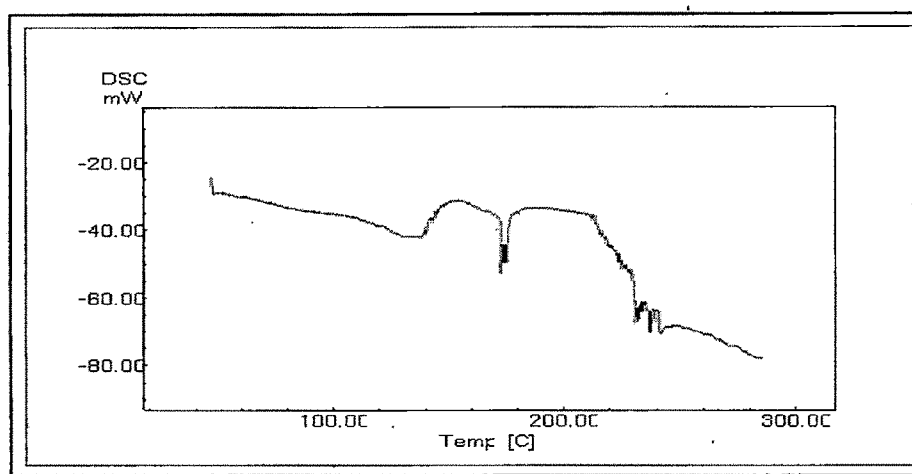


Figure 6.23: DSC thermogram of MTX

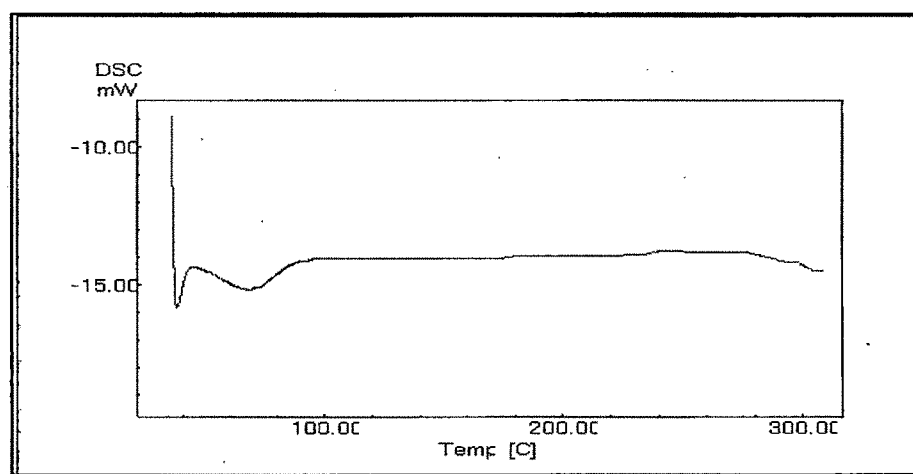


Figure 6.24: DSC thermogram of MSU-H MSNs

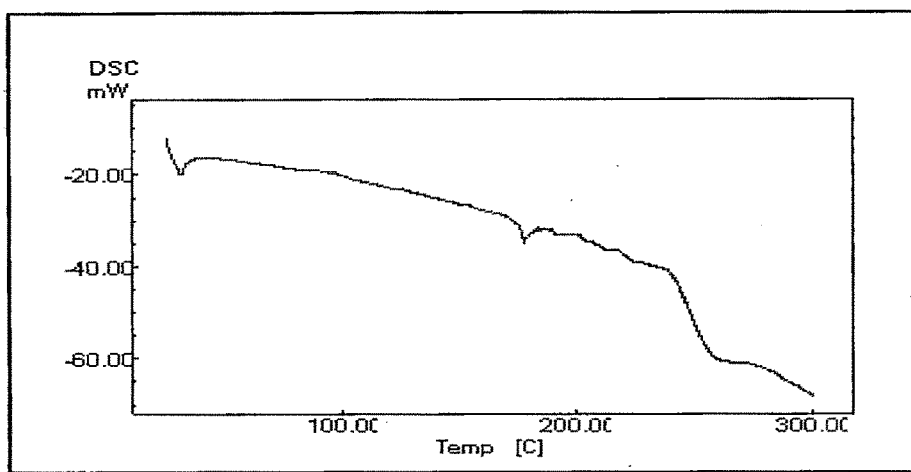


Figure 6.25: DSC thermogram of physical mixture of MTX and MSU-H MSNs

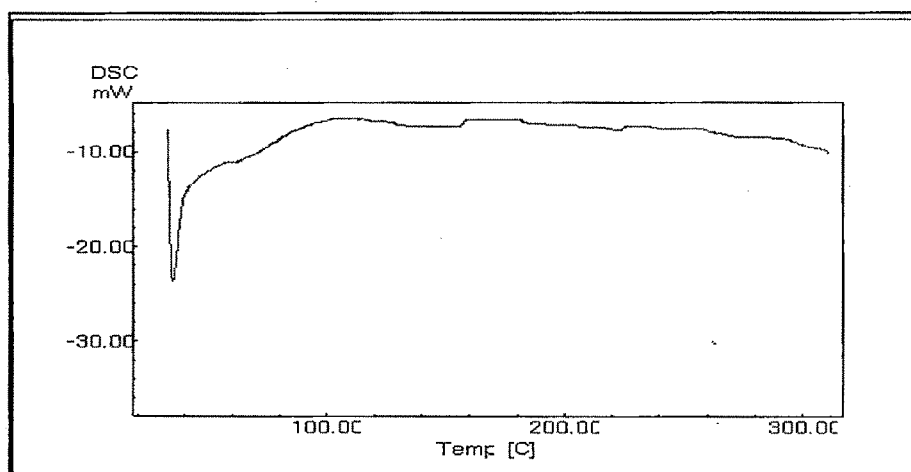


Figure 6.26: DSC thermogram of MTX loaded MSU-H MSNs

Fig. 6.23-6.26 show DSC thermograms of MSU-H MSNs, drug loaded MSU-H MSNs, physical mixture, and crystalline MTX respectively. The DSC curve of MTX exhibited a single endothermic peak at 180 °C, which corresponded to its intrinsic melting points. Physical mixture of drug and MSNs show the less intense peak at 180 °C, indicated that drug molecules are not confined within the pores and drug was present in its crystalline state. However, no melting peak of MTX was identified in the DSC curves obtained from drug loaded MSNs. The absence of phase transitions owing to MTX in the DSC analysis is evidence that MTX is in a non-crystalline state.

6.6 *In-Vitro* dissolution study

Dissolution tests were performed at different pH conditions in order to investigate the drug release behavior in different regions of gastrointestinal tract. MTX dissolution from MSU-H-MTX was compared with those from MTX crystalline powder, physical mixture and marketed formulation (Fig. 6.28 (a–d)). In all test conditions MTX release from MSU-H MSNs had a more rapid burst effect than the pure powder, physical mixture and marketed formulation. Schematic presentation of drug release from MSU-H MSNs is shown in Fig. 6.27.

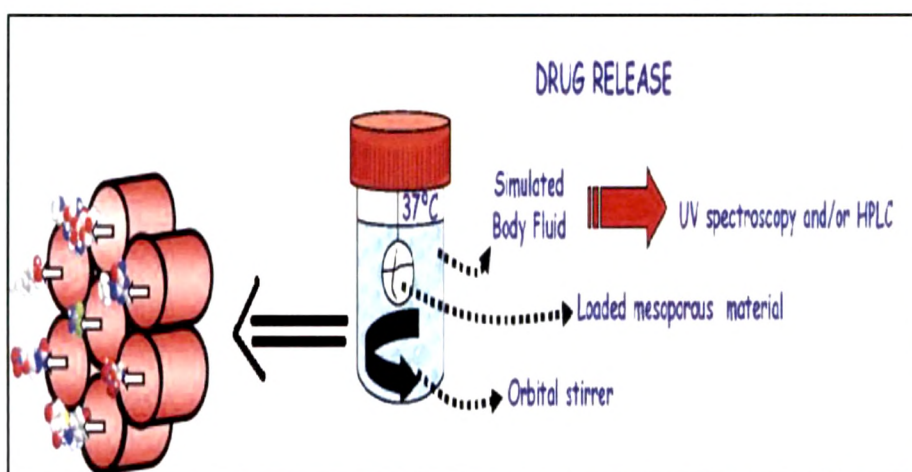


Figure 6.27: Schematic presentation of drug release from MSU-H MSNs

The dissolution improvement may be largely attributed to the pore channels of the carriers i.e. MSU-H MSNs, changing the crystalline state of MTX to an amorphous state, which is known to improve the drug solubility and dissolution rate¹⁵⁻¹⁷. In addition, the particle sizes of the amorphous drug incorporated in the pore channels (nano meter range) were significantly reduced compared with that of pure crystalline MTX (micron range). It is evident that a further decrease in the particle size to the nano meter range will further accelerate the drug release profile and, consequently, improve the dissolution rate^{15, 17, 18}.

Table 6.10 and 6.11 show the MTX release percentages at the tested pHs after 10 and 30 min respectively. It can be observed that differences in the release profile were more evident in gastric fluids. In fact, in pH 1.2 medium more than 60% and 95% of drug release was found from MSU-H-MTX after 10 and 30 min respectively. Whereas MTX dissolution from the crystalline powder was as low as 15% and less than 40% after 10 and 30 min respectively.

Table 6.10: Percentage of drug release after 10 minutes

Dissolution media	% drug release			
	Crystalline drug	Physical mixture	Marketed formulation	Developed formulation
Simul. gastric fluid pH 1.2	15.594	23.000	28.562	63.882
Phosphate buffer pH 4.5	14.843	20.876	24.607	58.350
Phosphate buffer pH 6.8	12.286	18.039	20.544	41.360
Simul.intest. fluid pH 7.4	11.941	16.025	16.983	39.325

Table 6.11: Percentage of drug release after 30 minutes

Dissolution media	% drug release			
	Crystalline drug	Physical mixture	Marketed formulation	Developed formulation
Simul. gastric fluid pH 1.2	36.701	65.595	79.697	96.451
Phosphate buffer pH 4.5	33.390	61.160	69.171	93.527
Phosphate buffer pH 6.8	31.712	58.956	58.848	88.977
Simul. Intest. fluid pH 7.4	29.729	51.008	57.287	85.970

Finally, the MTX dissolution profile from MSU-H-MTX at pH 1.2 was compared to that of MTX from commercial formulation. The dissolution profiles indicate that after the 10 min drug release was more than 60% from MSU-H-MTX whereas only 28% in comparison with market formulation. Similarly after 30 min drug release from marketed formulation was found to be 80% whereas more than 95% release was obtained from the developed formulation.

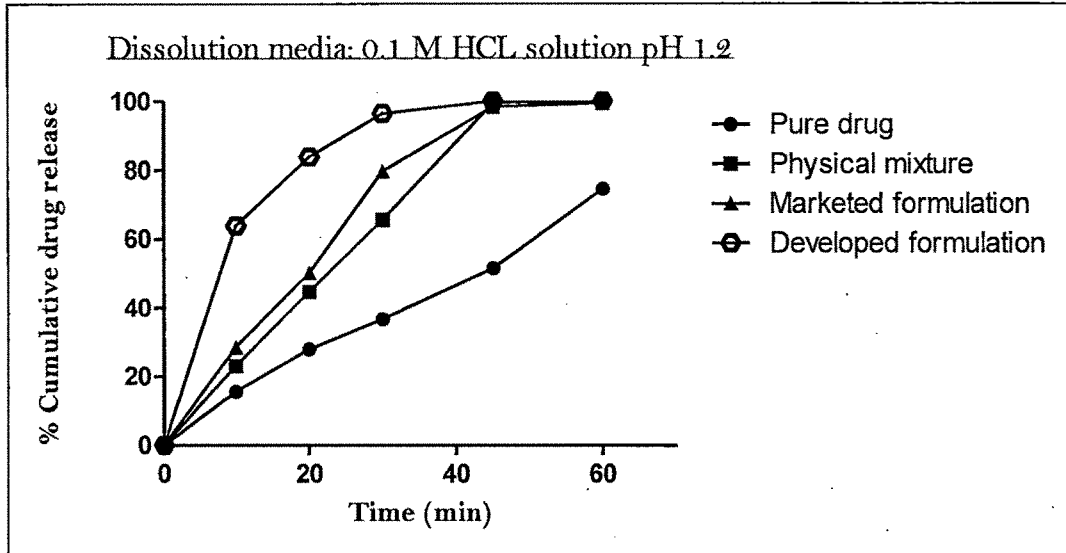


Figure 6.28-a: Release profile of MTX from crystalline MTX, physical mixture, marketed formulation, and developed formulation in pH 1.2

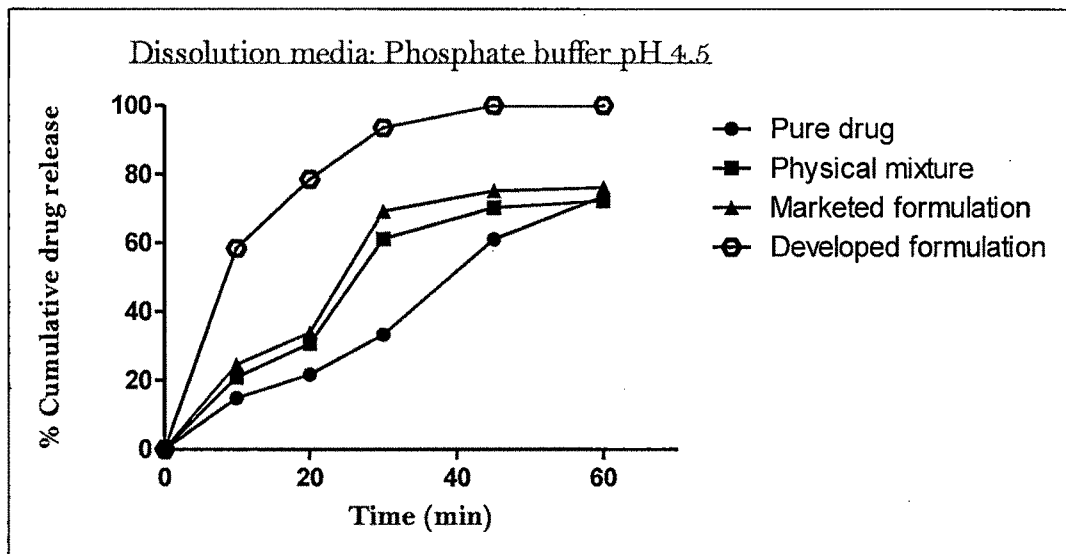


Figure 6.28-b: Release profile of MTX from crystalline MTX, physical mixture, marketed formulation, and developed formulation in pH 4.5

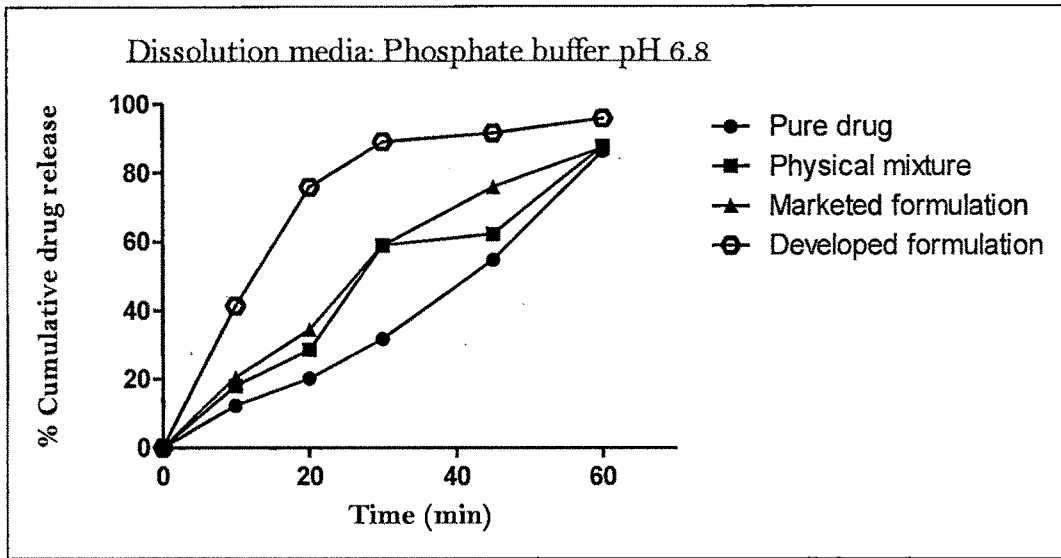


Figure 6.28-c: Release profile of MTX from crystalline MTX, physical mixture, marketed formulation, and developed formulation in pH 6.8

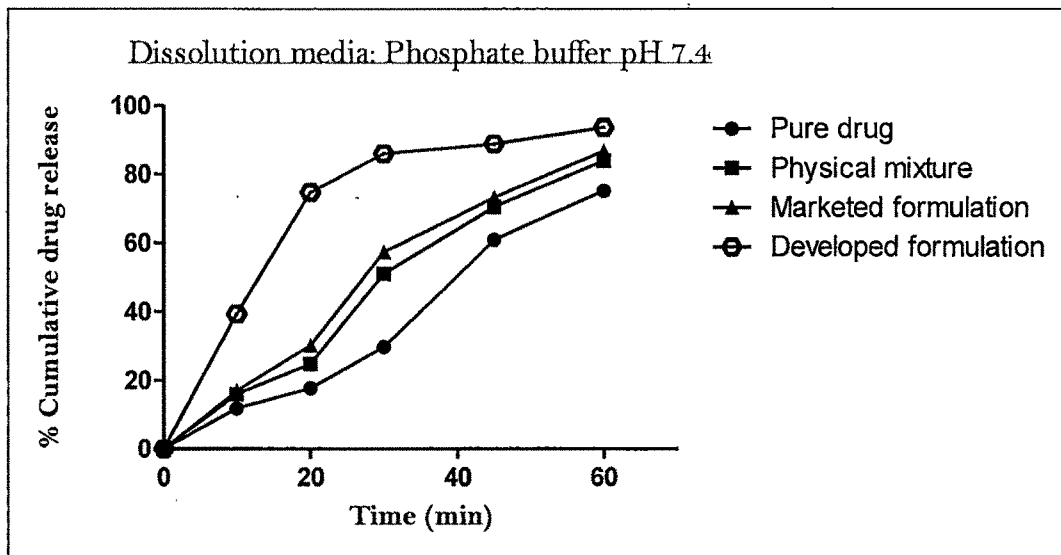


Figure 6.28-d: Release profile of MTX from crystalline MTX, physical mixture, marketed formulation, and developed formulation in pH 7.4

References:

- 1 Wujun Xu, Qiang Gao, Yao Xua, Dong Wu, Yuhan Sun, Wanling Shen, Feng Deng. Controllable release of ibuprofen from size-adjustable and surface hydrophobic mesoporous silica spheres. *Powd Tech.* 2009; 191: 13-20.
- 2 Seong SK, Karkamkar A, Pinnavaia TJ. Synthesis and characterization of ordered, very large pore MSU-H silicas assembled from water-soluble silicates. *J Phys Chem. B* 2001; 105: 7663-7670.
- 3 Prouzet E, Cot F, Boissie`re C, Kooymanb PJ, Larbota A. Nanometric hollow spheres made of MSU-X-type mesoporous silica. *J Mater Chem.* 2002; 12: 1553-1556.
- 4 Brunauer S, Emmet P, Teller E. Adsorption of gases in multi molecular layers. *J Am Chem Soc.* 1938; 60: 309-319.
- 5 Vallet RM, Balas F, Arcos D. Mesoporous materials for drug delivery. *Angew Chem Int Ed.* 2007; 46: 7548-7558.
- 6 Ida SC, Luigi P, Flaviano T, Rosario A, Francesco P, Francesca I, Nevio P. Silica based mesoporous materials as drug delivery system for methotrexate release. *Drug Del.* 2007; 14: 491-495.
- 7 Griesser U.J, The importance of solvates. In Hilfiker R, ed. *Polymorphism.* Wiley-VCH Verlag GmbH & Co. KGaA, Weinheim, 2006; 211-233.
- 8 CRC handbook of solubility parameters and other cohesion parameters, A. F. M. Barton, ed., 2nd ed., CRC Press cop, Boca Raton (FL), 1991.
- 9 Bhattachar SN, Deschenes LA, Wesley JA. Solubility: it's not just for physical chemists. *Drug Dis Today.* 2006; 11: 1012-1018.
- 10 Bennema P, Van J, Van W, Los JH, Meekes H. Solubility of molecular crystals: Polymorphism in the light of solubility theory. *Int J Pharm.* 2008; 351: 1-2, 74-91.
- 11 Vandervoort J, Ludwig A. Preparation factors affecting the properties of polylactide nanoparticles: a factorial design study. *Pharmazie.* 2001; 56: 484- 488.
- 12 Box G, Hunter W, Hunter J. *Statistics for experiments*, John Wiley and Sons, New York, 1978; 291-334.
- 13 Cochran W.G, Cox G.M. *Experimental Designs*, second ed., John Wiley and Sons, New York, 1992; 335-375.
- 14 Miguel M, Maria V. New developments in ordered mesoporous materials for drug delivery *J Mater Chem.* 2010; 20: 5593-5604.
- 15 Salonen J, Laitinen L, Kaukonen AM, Tuura J, Björkqvist M, Heikkilä T, Vähä-Heikkilä K, Hirvonen J, Lehto V.P. Mesoporous silicon microparticles for oral drug delivery: loading and release of five model drugs. *J Control Rel.* 2005; 108: 362-374.
- 16 Heikkilä T, Salonen J, Tuura J, Kumar N, Salmi T, Murzin D.Y, Hamdy M.S, Mul G, Laitinen L, Kaukonen A.M, Hirvonen J, Lehto V. Evaluation of mesoporous TCPSi, MCM-41, SBA-15, and TUD-1 materials as API carriers for oral drug delivery. *Drug Deliv.* 2007; 14: 337-347.

-
- 17 Vasconcelos T, Sarmiento B, Costa P. Solid dispersions as strategy to improve oral bioavailability of poor water soluble drugs. *Drug Discov Today*. 2007; 12: 1068–1075.
 - 18 Kesisoglou F, Panmai S, Wu Y. Nanosizing. Oral formulation development and biopharmaceutical evaluation. *Adv Drug Deliv Rev*. 2007; 59: 631–644.